Methodology for Travel Time Estimation on a Signalised Arterial

Ashish Bhaskar*, Edward Chung*, Olivier de Mouzon** André-Gilles Dumont*

** Traffic Facilities Laboratory (LAVOC), Swiss Federal Institute of Technology (EPFL), Lausanne, Switzerland*
***Traffic Engineering Laboratory (LICIT), French National Institute for Transport and Safety Research (INRETS), Lyon-Bron, France*

Abstract

This paper presents the development and testing of a methodology for estimation of average travel time on signalised urban networks. The methodology considers the classical analytical procedure, where average travel time on a study link is estimated as the average area between cumulative plots for the respective link. The challenge is to accurately estimate the plots based on the availability of data. The three different cases of data availability are considered: a) *case-D*, for only detector data; b) *case-DS*, for detector data and signal controller data; and c) *case-DSS,* for detector data, signal controller data and saturation flow rate. The performance of the methodology is evaluated under controlled environment considering different degree of saturation and different detection intervals. The performance for case-DS and for case-DSS is consistent whereas, the performance for case-D is highly sensitive to the signal phases in the detection interval.

Keywords: *Travel Time Estimation, Delay Estimation, Arterial Network, Urban Network*

1 Introduction

Traffic congestion is one of the inescapable conditions in almost all the cities. In Europe, the external social economic cost of congestion is estimated to be around 2 percent of the Gross Domestic Product, (Kinnock, 1995), which accounts to annual social loss of more than 120 billion euros. The increase in congestion on the road network results in more air and noise pollution, and in adverse physiological, psychological and social effects associated with it. It is almost impossible to eliminate peak hour congestion; however, efficient and intelligent management of traffic can reduce the congestion. Real time information of the performance of network is vital for intelligent traffic management. Travel time information quantifies the performance of the network and is one of the important performance measures for the transportation systems.

In the literature, different methodologies ranges from simple regression to more sophisticated artificial intelligence based algorithms are proposed. Most of the research on travel time estimation is limited to freeways (Zhang and Rice, 2003, Bajwa, 2003), where the spot speed and link speed can be easily correlated. However, travel time estimation on urban networks is more challenging. The presence of conflicting areas (intersections) whether signalised or non-signalised imposes delay that has a significant affect on travel time estimation.

Detectors are the widely used data sources and generally, in urban networks they are primarily used for signal control. There is increasing interest to use the detector data for travel time estimation. The earlier research on travel time estimation models via detector on signalised urban links is based on developing the regression relationship between detector occupancy and mean intersection delay with the use of traffic simulation modelling (Sisiopiku et al., 1994, Young, 1988, Xie et al., 2001) or real data (Zhang, 1999). Sisiopiku and Rouphail (1994) provide a review of earlier work on the use of detector output for travel time estimation. The regression analysis models provide a statistical relationship between input (occupancy, flow, green split) and output (travel time) without explicitly addressing the traffic processes that determine these travel times. These models are often site specific and require calibration of parameters for real application. The regression analysis is observed for detectors far from the stop-line and cannot be applied for stop-line detectors. The location and type of detector has significant influence on the methodology for travel time estimation. Location of the detector depends on the requirements of the signal control algorithm: for instance, SCATS signal control algorithms need data from the stop-line detector where as SCOOTS needs detector data at the upstream of the link. Stop-line detectors provide information for the vehicles that had passed the detector (or entered the intersection) and the queue left behind is unknown.

The proposed model integrates stop-line loop detector data with signal controller data and considers saturation flow rate. The model is expected to be a valuable tool for system performance evaluation and ITS applications such as Advanced Traveller Information Systems (ATIS) and dynamic route guidance. The performance of the

signalised intersection can provide a feedback to the signal controller to evaluate its effectiveness and optimise its parameters.

2 Travel time estimation model

The model considers classical analytical procedure of using cumulative plots for travel time estimation. In Figure 1, a single lane link (study link) between two consecutive intersections is shown. Travel time is defined as the time difference between the time when the vehicle enters the downstream intersection and the time when it entered the upstream intersection. The area (A), between cumulative plot at the upstream end of the link *($CP_{US}(t)$)* and cumulative plot at the downstream end of the link *($CP_{DS}(t)$)* provides the total experienced travel time for all the *N* number of vehicles which arrived during Δt time interval at the upstream end of the link. Average travel time per vehicle is the ratio between total area and number of vehicles arrived.

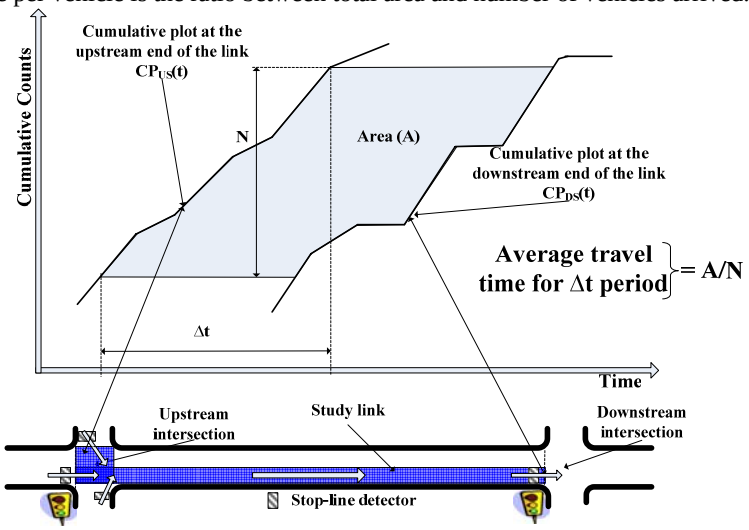

Figure 1: Analytical methodology for travel time estimation.

In this research, it is assumed that there is no shared lane and the stop-line detectors are present on all the lanes that contribute to cumulative plots. Stop-line loop detectors, provide aggregated counts and occupancy during detector detection interval. Signal controller provides real time signal parameters such as signal phase plan and start time and end time of each phase. Actually, signal controller provides the green and red time for each phase. The corresponding effective green and effective red time are estimated by considering initial loss time and end gain time. In the remaining part of the paper the use of terms *green* and *red* should be considered as *effective green* and *effective red*. Saturation flow rate is a parameter specific to each site under study. It is determined for each lane group at the intersection and depends on factors such as road geometry and environmental conditions.
To generalise the model, cumulative plots at the location of the detector are estimated for the three cases depending on the availabilities of the data a) *Case-D:* Only detector data is available; b) *Case-DS:* Detector data and signal controller data is available and c) *Case-DSS:* Detector data, signal controller data and saturation flow rate is available. The slope of the plot defines the flow pattern at the respective entrance of the intersection.
We define N_d and q as the counts and flow, respectively during the detection interval of *DI* seconds.

Case-D: If only detector data is available then it is assumed that the counts during a detection interval are from a flow pattern (eqn (1)) that is uniformly distributed throughout the detection interval (Figure 2a). The assumption is reasonable for lower detection intervals and in the absence of any further information can be applied for higher detection interval.

$$q = \frac{N_d}{DI} \qquad (1)$$

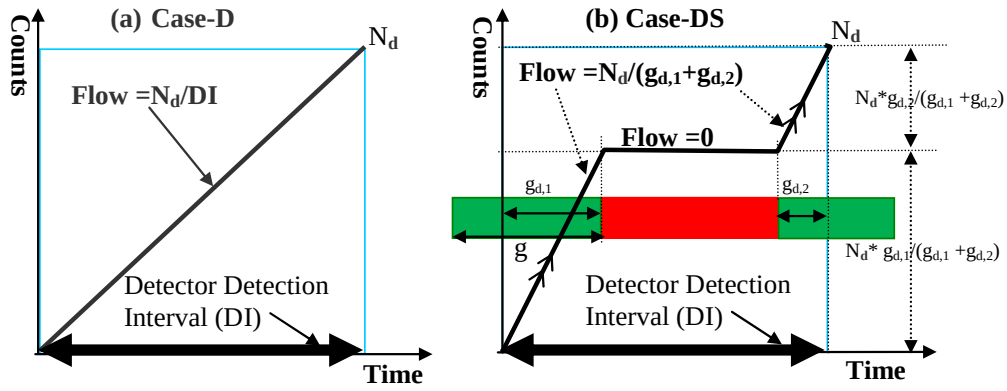

Figure 2: Flow pattern for (a) case-D and (b) case-DS.

Case-DS: If detector data and signal controller data is available then it is assumed that the counts during a detection interval are from a stepwise flow pattern (eqn (2)). Flow pattern is uniform only during the green period of the detection interval and during red period there is no flow (Figure 2b).This captures the fluctuations in the flow pattern even for higher detection interval. We define $g_{d,i}$ as the *i-th* green interval during the detection interval In Figure 2b, two green periods are present during the detection interval and the counts are distributed to each green interval in proportion to the corresponding green time. Flow pattern during each green periods of the detection interval are parallel to each other.

$$q = \frac{N_d}{\sum g_{d,i}} \quad during\ green\ period\ in\ detection\ interval$$
$$= 0 \quad during\ red\ period\ in\ detection\ interval \qquad (2)$$

Case-DSS: We define the demand, which should be the cumulative plot *(CP_{demand})* at the location of the stop-line detector if there was no restriction, at the intersection, on the flow of the vehicles.
At a signalised intersection, during the green phase, the vehicles from the queue are effectively discharged at saturation flow. Thereafter, the flow pattern follows the demand pattern. If demand and saturation flow are known then more accurate flow pattern considering saturation flow and non-saturation flow can be estimated.
The count, N_i, during each *i-th* green period ($g_{d,i}$) in the detection interval is assumed to be in proportion to $g_{d,i}$ (eqn (3)).

$$N_i = \frac{N_d * g_{d,i}}{\sum_i g_{d,i}} \qquad (3)$$

For simplicity, we focus on green (*g*) for a complete signal cycle instead $g_{d,i}$. The *g* can extend in more than one detection interval. For instance, in Figure 2b, the g has the component $g_{d,1}$ during the detection interval indicated in the figure. The count, N_g, during *g* is obtained by respective adding the counts from all its components, if splitted in more than one detection intervals.
The maximum number of vehicles which can depart during *g* is $N_{max}(=s*g)$, where *s* is saturation flow rate (vehicles/second). Out of N_g vehicle, n_s number of vehicles enters the intersection at saturation flow pattern and the remaining (N_g-n_s) follow the demand pattern.
For a link between two consecutive intersections as shown in Figure 1, the demand pattern, for the detector at the downstream end of the link, can be estimated from $CP_{US}(t)$. However, for a network there can be certain links where the $CP_{US}(t)$ is unknown such as at the entrance of the network. Therefore, the following two cases of unknown or know demand pattern are considered to estimate cumulative plots for case-DSS.
(a) Unknown demand pattern: The detector counts represent demand for under-saturated and saturated situations. However, for over-saturated situation, the counts are upper bounded by capacity and that may be less than true demand. Therefore, demand estimated in this case is termed as "assumed demand".
The demand flow pattern can be assumed to follow a uniform pattern (deterministic) or can be assumed to be distributed according to some probability distribution (stochastic). To simplify the analysis it is assumed that demand is uniform during the signal cycle. As shown in Figure 3, N_g numbers of vehicles are counted during the green phasethat represents the uniform demand for the signal cycle. By superimposing saturation flow pattern (during the green phase) on the uniform demand pattern the following relationship can be geometrically obtained:

$$\frac{n_s}{N_g} = \frac{(1 - g/C)}{(1 - \frac{N_g}{N_{max}}\frac{g}{C})} \quad for\ N_g \le N_{max}$$
$$= 1 \quad for\ N_g > N_{max} \qquad (4)$$

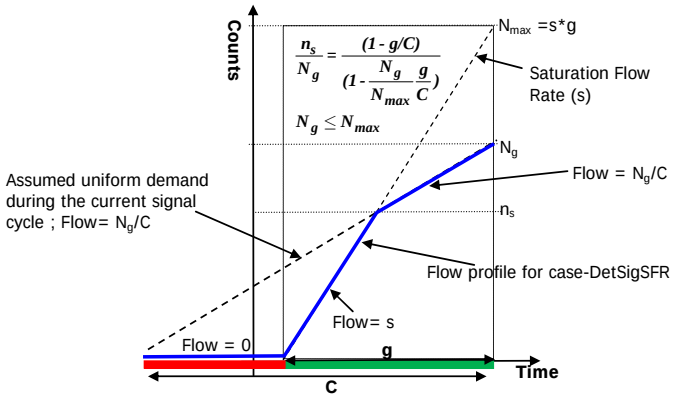

Figure 3: Geometrical relationship between n_s and N_g assuming uniform demand pattern during the current signal cycle.

On average demand should never be greater than capacity so, $N_g > N_{max}$ should not be possible. However, during certain intervals it is possible that the flow rate exceeds the defined saturation flow rate. Hence, the model is defined for $N_g > N_{max}$, in which all the vehicles enter the intersection at saturation flow rate.
The detector counts represent demand for under-saturated and saturated situations however, for over-saturated situation, the counts are equal to capacity and that may be less than true demand. Hence, for under-saturated and saturated situations, the ratio N_g/N_{max} represents degree of saturation and n_s/N_g is the percentage of demand in saturation flow rate. Eq(4) provides the ratio of the counts in saturation flow rate to the total counts. For a given demand, the higher the green split (g/C) lower the n_s/N_g ratio; and for near to saturated situations the ratio is close to one. This is as expectation, because as the demand approaches capacity almost all the vehicles are at saturation flow rate. This relationship is represented as graphs in Figure 5 for different green splits.

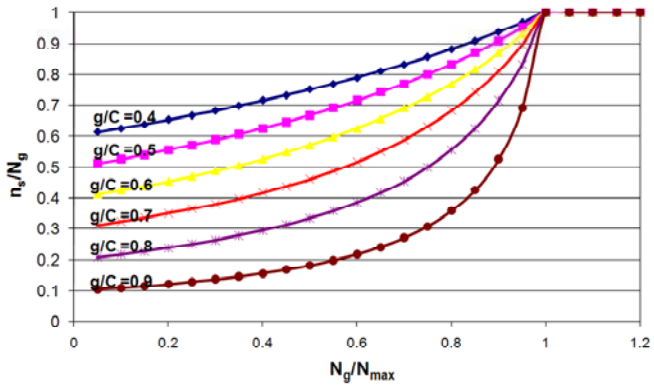

Figure 4: Relationship between n_s/N_{max} for different counts and green split.

(b) Known demand pattern: In this case, we are interested to estimate $CP_{DS}(t)$, given $CP_{US}(t)$. The $CP_{demand}(t)$ is the horizontal shift of the CP_{US} by free-flow travel time $(tt_{freeflow})$ of the link i.e., $CP_{US}(t\text{-}tt_{freeflow})$. The demand is deduced from the upstream cumulative plot, so we call this demand as "deduced demand". It is assumed that the vehicle counts during the detection interval are from a step-wise flow pattern. The flow is zero for red intervals and for green interval if CP_{demand} is greater than the cumulative counts ($CP_{DS}(t)$) then the flow is at saturation flow otherwise, the flow pattern is same as demand pattern (see eqn (5)).

During Red Period

$q = 0$

During Green Period

if $CP_{demand}(t) > CP_{DS}(t)$

$q = s$

else

$$q = \frac{\partial CP_{demand}(t)}{\partial t} \qquad (5)$$

As shown in Figure 5, the upstream cumulative plot, $CP_{US}(t)$, and the number of vehicles departing from the downstream end of the link (N) are known and flow pattern at downstream intersection for the current detection interval is unknown. The required flow pattern during the current detection interval is obtained by no flow during red period (a to b) and during green period, the flow is at saturation flow pattern until demand pattern intersects the saturation flow pattern (b to c) and thereafter flow follows the demand pattern (c to d).

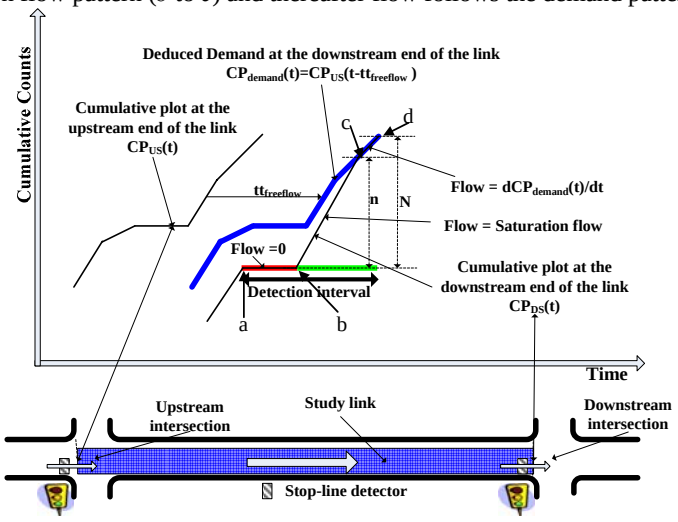

Figure 5: Flow pattern at downstream end of the link for case-DSS.

2.1 Variability of travel time

The model provides average travel time during Δt time interval. One can argue that the average travel time is the performance measure for the system; however, it may not be a true representative of the travel time experienced by an individual vehicle. The variability of the individual vehicle travel time during Δt time interval can provide a confidence interval for the travel time estimate. The variability is obtained by fragmenting the total area A (Refer to Figure 1) as discussed below.

We define cumulative plot, *CP,* as a polyline with *MCP* as the matrix of nodes for the polyline. The total area A, is fragmented into different areas (A_i) (refer to Figure 6), by horizontal cuts correspond to the nodes at MCP_{US} and MCP_{DS} and with the following constraint: For each fragmented area, A_i, if the counts, N_i, are above a certain threshold number, $N_{threshold}$, then the time interval for the arrival, t_{usi}, and departure, t_{dsi}, corresponding to the fragmented area should be under a certain threshold time interval ($t_{threshold}$). If not, then the area (A_i) is further fragmented by a horizontal cut to satisfy the constraints. The process is repeated until each fragmented area satisfies the constraints.

Finally, each fragmented area (A_i) represents the total travel time for the N_i number of vehicles in the respective areas. Assuming that these N_i numbers of vehicles experience more or less similar travel time, the variability is obtained by the following equation:

$$\overline{TT} = \frac{\sum_{i=1}^{m} A_i}{\sum_{i=1}^{m} N_i} = \frac{A}{N};$$

$$\overline{TT_i} = \frac{A_i}{N_i};$$

$$\sigma^2 = \frac{\sum_{i=1}^{m} (\overline{TT_i} - \overline{TT})^2 N_i}{m-1} \qquad (6)$$

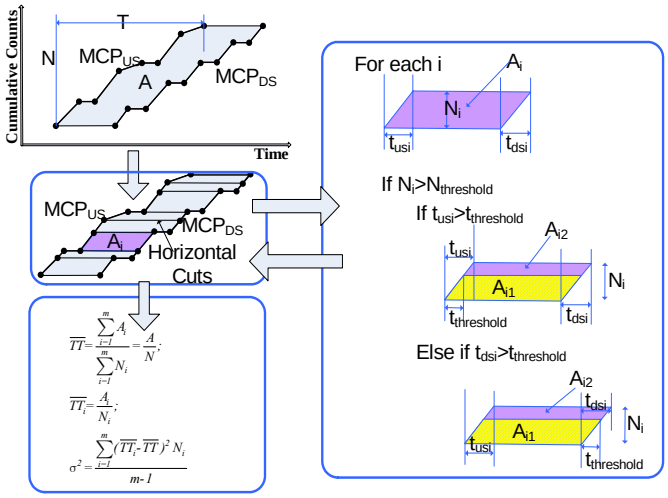

Figure 6: Flowchart for variability estimation.

3 Model testing on controlled environment

To test the methodology described in the previous section a computerized model for travel time estimation is developed and is linked with a microscopic traffic simulator, AIMSUN(Barcelo et al., 2005). The use of simulation software for research is increasing, as they can efficiently represent the real world situation and reproduce its behaviour. For realistic representation of the network and reproduction of the network behaviour, the parameters for simulation model need to be calibrated. For a calibrated network, different scenarios can be simulated and the methodology can be tested for each scenario.
The three different AIMSUN API modules used in this research are for extraction of a) signal controller data i.e., signal phases and its corresponding time b) detector data i.e., detector counts and occupancy for each detection interval and c) individual vehicle travel time. Detector data and signal data are inputs to the model for travel time estimation, which estimates average travel time for different intervals. Finally, the model is validated by comparing the average travel time estimated with the actual average travel time obtained from the individual vehicle API module.

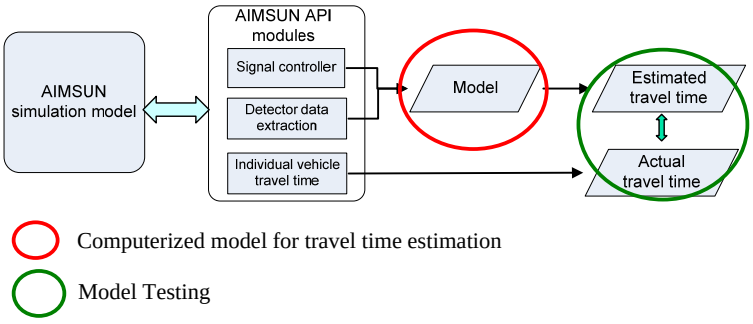

Figure 7: Framework for testing the proposed model using AIMSUN simulation model

3.1 Test Bed and simulation conditions

For simplicity only through movement at downstream intersection is considered. For upstream intersection the flow from three different directions are considered as shown in Figure 8. Both the upstream and downstream intersections are signalised with bottleneck at the downstream intersection. To consider different degrees of saturation for the study link, different demands on the upstream intersection are simulated. Scenarios for different degrees of saturation in the range of 0.5 to 1.2 are simulated with 10 replications each. For each scenario, the simulation is performed for an hour and average travel time for 6 minutes is considered. The sensitivity analysis for the model is performed for a fixed signal cycle of 120 seconds and detector detection interval from 10 to 360 seconds.

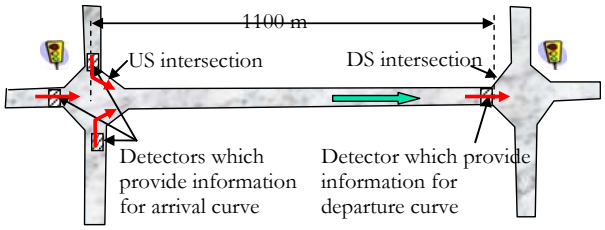

Figure 8: Test bed for the simulation.

3.2 Simulation test results

The performance of the model is defined in terms of accuracy (%) as follows:

$$Accuracy(\%) = (1 - \frac{\sum_{i=1}^{N} \frac{|actual_i - estimated_i|}{actual_i}}{N}) * 100 \quad (6)$$

Where, N is the total number of time intervals. $Actual_i$ and $estimated_i$ are the average actual travel time and average estimated travel time for each time interval, respectively.

Figure 9 represents the graphs for detector detection intervals versus accuracy for the three cases. As expected, lower detection intervals have higher accuracy levels irrespective of the cases and for detection interval less than 30 seconds the estimation is very accurate. Detection interval is not critical if signal timings are available. Comparable accuracy can be obtained from a) detector data from larger detection interval with signal timings and b) detector data from shorter detection interval without signal timings. If detection interval is short, then signal controller data and saturation flow rate is not necessary. For case-D, the performance is not consistent for different detection intervals and the accuracy around 80% when detection interval is close to integral multiple of signal cycle for instance 120, 240 and 360 in this example. This inconsistency in the performance for case-D is analysed in the next subsection.

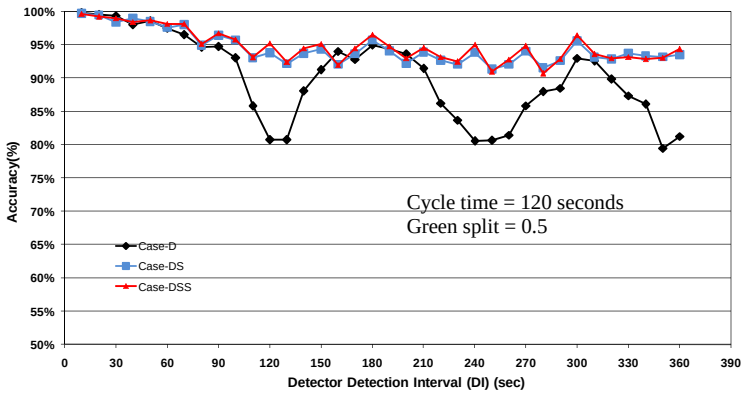

Figure 9: Detector detection interval versus accuracy.

The methodology to estimate of travel time variability presented in section 2.1 can provide reliable estimate only if cumulative plots are estimated accurately. Detector data from larger detection intervals with signal timings or detector data with shorter detection intervals have the flexibility to capture the randomness in the flow profiles and hence can be applied to estimate the variability. Figure 9, represents the graphs for actual versus estimated travel time variability for the three cases under different detection interval. For lower detection interval, the estimation of variability is accurate for all the cases. However, for case-D under higher detection interval (Figure 9c) the estimated variability has significant deviation from that of actual variability.

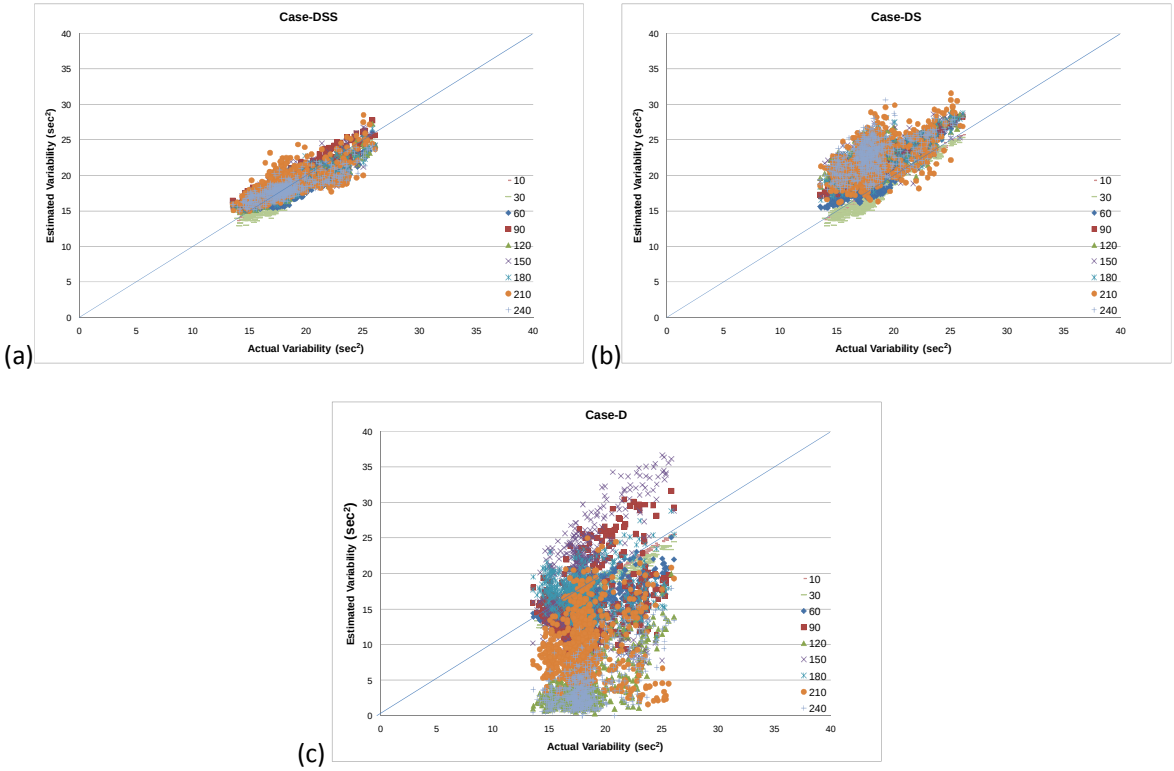

Figure 10: Actual versus estimated travel time variability for three cases and different detection interval.

4 Fundamental analysis for case-D and discussions

Fluctuations in the flow from certain combinations of signal phases in the detection interval can result in significant error in the travel time estimation from the cumulative plots generated under case-D. To study this, a detection interval equal to signal cycle is considered. Four different combinations of signal phases in the detection interval are possible: a) RG combination: red period followed by green period; b) GR combination: green period followed by red period; c) RGR combination: green period between two red periods; and d) GRG combination: red period between two green periods. As demonstrated in Figure 11, for case-D, the $CP_{US}(t)$ estimated for (a) RG combination has tendency to overestimate travel time and (b) GR combination has tendency to underestimate travel time. Whereas, in Figure 12, the $CP_{DS}(t)$ estimated based on: (a) RG combination has tendency to underestimate travel time and (b) GR combination has tendency to overestimate travel time. For RGR combination, the estimation for both $CP_{US}(t)$ and $CP_{DS}(t)$ profiles can be either underestimated, overestimated or exact.

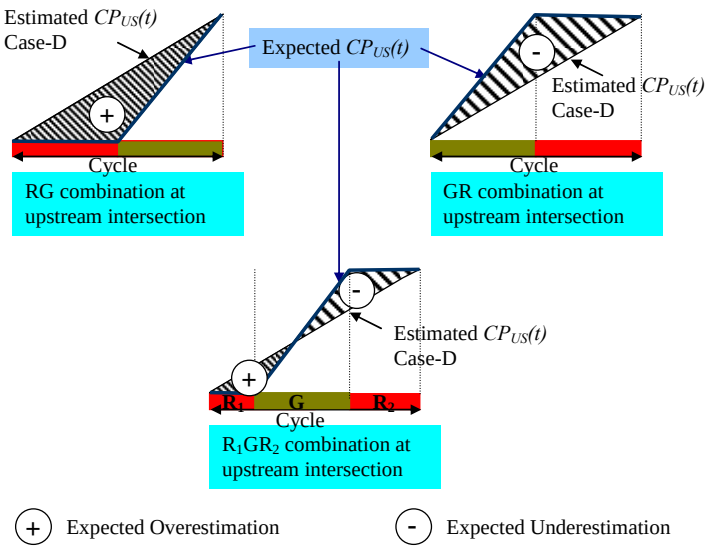

Figure 11 $CP_{US}(t)$ profile with detector detection interval equal to signal cycle at upstream intersection

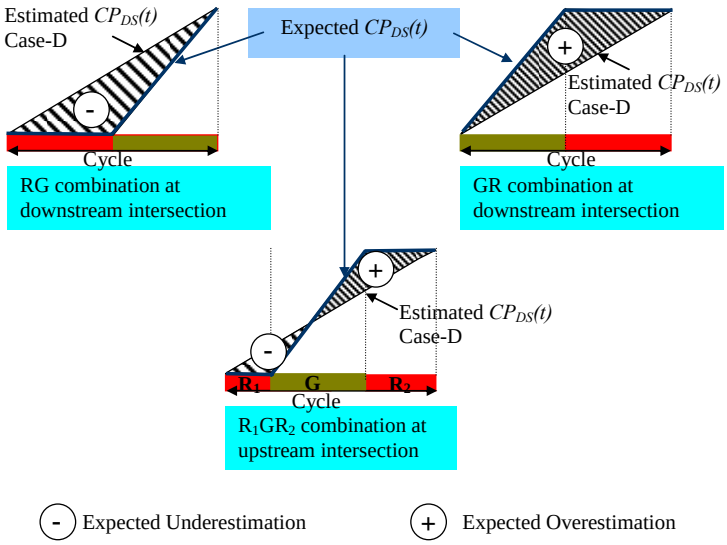

Figure 12 $CP_{DS}(t)$ profile with detector detection interval equal to signal cycle at downstream intersection

Figure 13 represents graph of actual average travel time versus estimated average travel time obtained from simulating following four different combinations of signal phases in the detection interval: a) RG_GR (++) combination b) GR_RG (--) combination c) GR_GR (-+) combination and d) RG_RG (+-) combination. Here, RG_GR (++) combination represents red phase followed by green phase in the detection interval at upstream intersection whereas, green phase followed by red phase in the detection interval at downstream intersection and so for others.

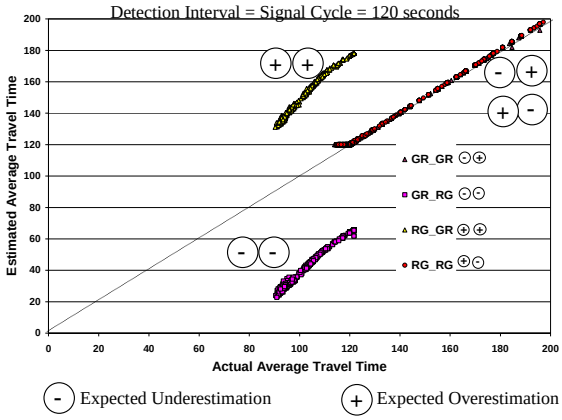

Figure 13: Performance for case-D under different combination of signal phases in the detection interval.

The RG_GR (++) combination has the tendency to highly overestimate travel time. Conversely, GR_RG (--) combination has the tendency to highly underestimate travel time. In the present example, the GR_GR (-+) and RG_RG (+-) combinations results in exact estimation because the underestimate travel time at upstream is compensated by the overestimate travel time at downstream and vice versa.

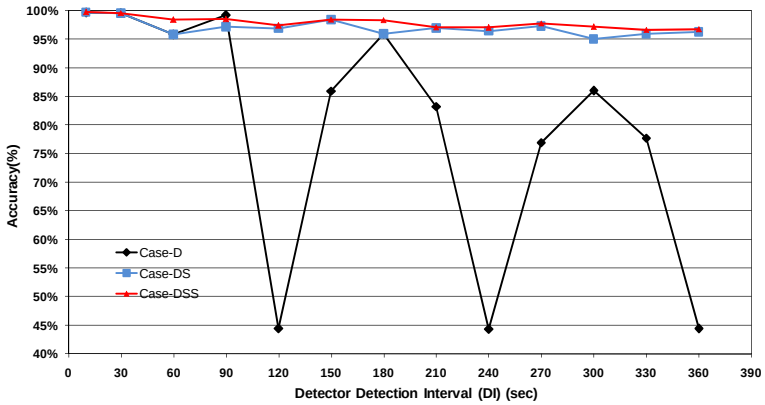

Figure 14: Detector detection intervals versus accuracy graphs for the three different cases of data availability with GR_RG (--) combination.

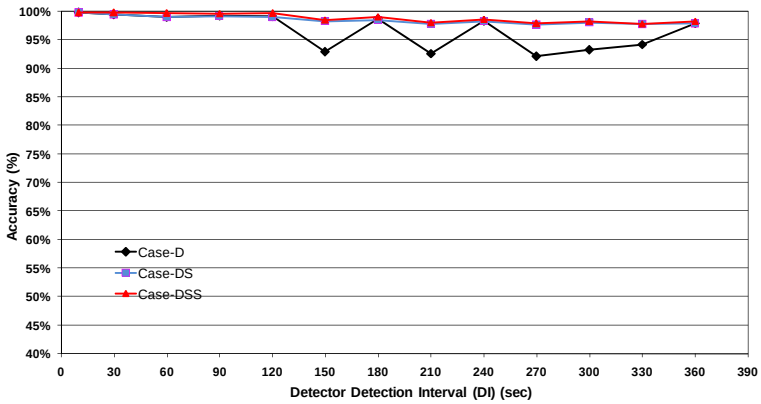

Figure 15: Detector detection intervals versus accuracy graphs for the three different cases of data availability with GR_GR (-+) combination.

Figure 14 and Figure 15 presents the detector detection intervals versus accuracy graphs for the three different cases for GR_RG(--) combination and GR_GR (-+) combination, respectively. The performance for case-D is highly sensitive to the signal phases in the detection interval. When detection interval is integral multiple of signal cycles (120 sec, 240 sec and 360 sec) then there is huge inconsistency in travel time estimation for case-

D. This means that when only detector data is available, detection interval should be carefully chosen in order to provide reliable travel time information from this data. The performance for case-DS and case-DSS is consistent and is not sensitive to the signal phases in the detection interval. The accuracy is generally more than 95% and is within the acceptable limits. The integration of detector data with signal controller has the potential to improve the accuracy with better confidence in estimation.

5 Conclusions and further research directions

The model provides a reliable and good estimate for average travel time on a link between two consecutive signalised intersections. The performance of the model for case-DS and case-DSS is consistent for different detection intervals with the accuracy generally more than 95%. However, if only detector data is available (case-D) then the error in the estimation is not consistent with different detection intervals. If the detection interval is close to integral multiple of signal cycle then the estimation can be very accurate or can have a significant error. The fundamental analysis for case-D with such uncertainty is also provided. For case-D, what matters is not how frequent the data is collected, but how the detection interval is related to signal timings. For instance, if signal cycle is two minutes and data is collected for four minutes interval then one can argue that for better confidence in travel time estimation one can collect the data for five minutes instead of four minutes which is twice the signal cycle.
The results from the test of the model on a simulated network are encouraging, and the extension of the model to estimate travel time for different movements on the link is under development.

6 References

BAJWA, S. U. I. (2003) Short-term travel time prediction using traffic detector data. *Department of Civil Engineering, Faculty of Engineers.* Tokyo, Japan, University of Tokyo.

BARCELO, J., CODINA, E., CASAS, J., FERRER, J. L. & GARCIA, D. (2005) Microscopic traffic simulation: A tool for the design, analysis and evaluation of intelligent transport systems. *Journal of Intelligent and Robotic Systems: Theory and Applications,* 41**,** 173-203.

KINNOCK, M. N. (1995) Towards fair and efficient pricing in transport: Policy options for internalising the external costs of transport in the European Union. European Commission Directorate-General For Transport-DG VII.

SISIOPIKU, V. P. & ROUPHAIL, N. M. (1994) Toward the use of detector output for arterial link travel time estimation: a literature review. *Transportation Research Record***,** 158-165.

SISIOPIKU, V. P., ROUPHAIL, N. M. & SANTIAGO, A. (1994) Analysis of correlation between arterial travel time and detector data from simulation and field studies. *Transportation Research Record***,** 166-173.

XIE, C., CHEU, R. L. & LEE, D. H. (2001) Calibration-free arterial link speed estimation model using loop data. *Journal of Transportation Engineering,* 127**,** 507-514.

YOUNG, C. P. (1988) A relationship between vehicle detector occupancy and delay at signal-controlled junctions. *Traffic Engineering and Control,* 29**,** 131-134.

ZHANG, H. M. (1999) Link-journey-speed model for arterial traffic. *Transportation Research Record***,** 109-115.

ZHANG, X. & RICE, J. A. (2003) Short-term travel time prediction. *Transportation Research Part C: Emerging Technologies,* 11**,** 187-210.